Constitutively active STAT5b feminizes mouse liver gene expression

Dana Lau-Corona[1], Hong Ma[1], Cameron Vergato[1], Andre Sarmento-Cabral[2], Mercedes del Rio-Moreno[2], Rhonda D Kineman[2], David J Waxman[1]

[1] Department of Biology and Bioinformatics Program
Boston University, Boston, MA

[2] Department of Medicine, Section of Endocrinology, Diabetes, and Metabolism, University of Illinois at Chicago and Research and Development Division, Jesse Brown VA Medical Center, Chicago, IL

Key words: Liver sex differences, STAT5 knockout, pituitary GH secretion profiles, JAK-STAT

Running title: Feminization of liver by STAT5b$_{CA}$

Supported in part by NIH grant DK121998 (to DJW) and grants NIH DK114326 and VA Merit BX005382 (to RK)

Address correspondence to:

Dr. David J. Waxman
Dept. of Biology
Boston University
5 Cummington Mall
Boston, MA 02115 USA
Email: djw@bu.edu

Abstract

STAT5 is an essential transcriptional regulator of the sex-biased actions of growth hormone (GH) in the liver. Delivery of constitutively active STAT5 (STAT5$_{CA}$) to male mouse liver using an engineered adeno-associated virus with high tropism for the liver is shown to induce widespread feminization of the liver, with extensive induction of female-biased genes and repression of male-biased genes, largely mimicking results obtained when male mice are given GH as a continuous infusion. Many of the gene expression changes observed were associated with STAT5 binding to liver chromatin, supporting the proposed direct role of persistently active STAT5 in continuous GH-induced liver feminization. The feminizing effects of STAT5$_{CA}$ were dose-dependent; moreover, at higher levels, overexpression of STAT5$_{CA}$ resulted in some histopathology not seen in continuous GH-infused male liver, including hepatocyte hyperplasia and distorted liver architecture. These findings establish that the persistent activation of STAT5 by GH that characterizes female liver is by itself sufficient to account for the female-biased expression of a majority of female-biased genes. Moreover, histological changes seen when STAT5$_{CA}$ is overexpressed highlight the importance of carefully evaluating such effects before considering such STAT5 derivatives for therapeutic use in treating liver disease.

Introduction

Sex-differences in pituitary growth hormone (GH) secretory patterns control the sex-biased expression of hundreds of genes in mouse liver (1) and contribute to the sexual dimorphism of liver physiology and pathology (2,3). In males, GH is secreted as a series of intermittent pulses followed by extended periods when circulating GH is undetectable, whereas in females, GH secretion is near continuous (1,4). Sex differences in liver gene expression are largely abolished when pituitary GH secretion is ablated by hypophysectomy, and can be substantially restored when exogenous GH is administered as a series of pulses (male circulating GH pattern), which confers a male pattern of expression, or as a continuous infusion (female GH pattern), which results in a female pattern of expression (5,6).

GH binding to its cell surface receptor activates the receptor-bound tyrosine kinase JAK2, which in turn phosphorylates and thereby activates the latent cytoplasmic transcription factor STAT5 (7,8). GH receptor/JAK2-activated STAT5 dimerizes and translocates to the nucleus, where it binds to thousands of sites in liver chromatin and induces transcription of many target genes (9,10). STAT5b, the major liver STAT5 form, plays a crucial role in liver metabolism and is an essential transcriptional regulator of the sex-dependent actions of GH in the liver (11,12). In male liver, repeated pulses of hepatic STAT5 activity, nuclear localization and transcriptional activity are observed and closely track the successive pulses of male pituitary gland GH release (13-15), whereas in female liver, STAT5 is persistently activated by the near-continuous female plasma GH profile (9,16). In whole body STAT5b knockout male mice, 90% of hepatic male-biased genes are repressed and 60% of hepatic female-biased genes are de-repressed (i.e., induced) (11). Further, STAT5 binds in a sex-biased manner to several thousand sites in mouse liver chromatin, with the set of male-biased STAT5 binding sites enriched nearby genes showing male-biased expression and the set of female-biased binding sites enriched nearby female-biased genes (9,17). Recent studies in a hepatocyte-specific STAT5a/STAT5b-KO mouse model (18) confirm these findings (19), supporting the proposal that the loss of hepatic STAT5, rather than an indirect feedback response to the loss of STAT5 in the hypothalamus or the pituitary gland, is responsible for the loss of liver sexual dimorphism seen in global STAT5b knockout mice.

Continuous infusion of GH in male mice (cGH treatment) substantially feminizes liver gene expression (20,21), most likely by a combination of two mechanisms. First, cGH overrides the endogenous male pulsatile plasma GH profile. This leads to widespread repression of male-biased genes that are positively regulated by male plasma GH pulses (class I male-biased genes) and to de-repression of female-biased genes that are negatively regulated by male GH pulses (class II female-biased genes) (22). Second, cGH treatment imposes a persistent, female-like pattern of plasma GH stimulation on male liver, which leads to the induction of female-biased genes that are positively regulated by the endogenous female GH pattern (class I female-biased genes) and represses male-biased genes that are negatively regulated by the female GH pattern (class II male-biased genes) (15,22). GH-activated STAT5 is a strong transcriptional activator of its well established direct target genes, including *Igf1* and *Socs2* (10,23), and similarly, can directly activate at least some class I male-biased genes when it is activated by a plasma GH pulse in male mouse liver (15). However, it is uncertain whether STAT5 signaling directly regulates other classes of sex-biased genes, most notably class I female-biased genes, which require a female plasma GH pattern for expression, or alternatively, whether other GH-stimulated but STAT5-independent signaling pathways downstream of GH receptor and JAK2 (24-26) mediate their sex-dependent expression. The requirement of STAT5 for sex-biased hepatic expression of both class I and class II sex-biased genes (21) does not entirely resolve this question, given the apparent perturbation of feedback mechanisms leading

to changes in circulating GH patterns seen in both STAT5 knockout and GH receptor-deficient mouse models (18,27).

Here, we address these questions using AAV8-STAT5$_{CA}$, a novel adeno-associated virus (AAV) vector that we engineered to deliver STAT5b with a point mutation in its SH2 domain (STAT5b Asn-642 to His) (28). This mutation renders the STAT5 protein constitutively active ('CA') and thus able to support robust expression of hepatic *Igf1* in the absence of GH (29). AAV8-STAT5$_{CA}$ is based on AAV serotype 8, which has high specificity for infection of hepatocytes (30,31). Moreover, the STAT5b mutant is expressed from the hepatocyte-specific thyroxin-binding globulin promoter, which confers additional specificity for persistent expression of the constitutively active STAT5 in hepatocytes. We hypothesized that the persistent expression of active STAT5 protein in male mouse liver mimics the persistent activation of liver STAT5 seen in female liver and will feminize gene expression. Our findings reveal that the delivery of STAT5$_{CA}$ to male mouse liver leads to widespread induction of female-biased genes and repression of male-biased genes, and thus feminization of the liver by persistent plasma GH stimulation can largely be attributed to the persistent activation of liver STAT5b.

Materials and Methods

Preparation of AAV8-STAT5$_{CA}$ - Wild-type mouse STAT5b expression plasmid with an N-terminal Flag tag was obtained from SinoBiological, Wayne PA (cat. # MG51116-NF). A point mutation at base 1963 (A to C), which changes Asn642 to His, was introduced into the STAT5b coding sequence by Genscript (Piscataway, NJ). This mutation confers constitutive activity (CA) to STAT5b, including the ability to induce *Igf1* gene expression in livers of hypophysectomized (GH-deficient) rats (28,29). The mutated plasmid was sent to Penn Vector Core (University of Pennsylvania, Philadelphia, PA), where the N-Flag-mSTAT5b$_{CA}$ cDNA was cloned into the Penn Vector Core plasmid pENN.AAV.TBG.PI.eGFP.WPRE.bGH, replacing eGFP by the mutated and tagged STAT5b$_{CA}$. The resultant plasmid, pENN.AAV.TBG.PI.N-FLAG-mSTAT5bCA.WPRE.bGH, was sequence verified then packaged in AAV8 virus, which was purified, quantified with respect to genome copy (GC) number, and supplied by Penn Vector as a ready to use vector, AAV8-TBGp-mStat5b$_{CA}$, referred to here as AAV8-STAT5$_{CA}$. The plasmid pENN.AAV.TBG.PI.N-FLAG-mSTAT5bCA.WPRE.bGH, required to prepare AAV8-STAT5$_{CA}$ (see lab methods, below), is being deposited and will be made available through Addgene (https://www.addgene.org/).

AAV8-STAT5$_{CA}$ expression in mouse liver. Initial studies to validate AAV8-STAT5$_{CA}$ were performed in male C57Bl/6 mice on a GHR$^{fl/fl}$ background at Jesse Brown VA Medical Center (Chicago, IL) with Institutional Animal Care and Use Committee approval (protocol number 19-05). AAV8-TBGp-Null vector (Penn Vector Core), referred to here as AAV8-Null, was used as a control. Male GHR$^{fl/fl}$ mice (10-12 wk, and maintained as an in-house breeding colony, originally provided by Dr. John Kopchick, Ohio University (32)) were injected via the lateral tail vein with AAV8-Null or AAV8-STAT5$_{CA}$ (1.5 x 10^{11} GC per mouse, diluted in sterile PBS). Seven days later the mice were decapitated, and livers were collected. Nuclear protein was extracted using NE-PER Nuclear Cytoplasmic Extraction Reagent (cat. # 78833, Pierce, Rockford, IL). Western blots were performed to detect the Flag-tag sequence using rabbit monoclonal anti-DYKDDDDK Tag antibody (Cell Signaling #14793). To test the efficacy of AAV8-STAT5$_{CA}$ to increase hepatic expression and restore circulating levels of IGF1 to normal levels, we used a mouse model with adult-onset hepatocyte-specific GH receptor knockdown (aHepGHRkd) (33), prepared as follows. Male GHR$^{fl/fl}$ mice (10-12 wk old) were injected via lateral tail vein with 1.5 x 10^{11} GC/mouse of either AAV8-Null, to obtain GH receptor-intact control mice, or AAV8 expressing

153 Cre recombinase (AAV8-TBGp-Cre, Penn Vector Core), to generate aHepGHRkd mice. The
154 above AAV8 injections done either alone or in combination with AAV8-STAT5$_{CA}$ (at 0.36 or 0.75
155 x 10^{11} GC), with the dose of AAV8-Null adjusted to equalize the total GC of AAV8 per mouse
156 across groups. Fourteen days later, blood and liver were collected to assay circulating IGF1
157 levels (Mouse/Rat IGF-1 ELISA, 22-IG1MS-E01, ALPCO) and liver IGF1 mRNA levels by qPCR
158 (33). In other studies, GH receptor-intact male mice (C57Bl/6 strain from Jackson Labs, 10 wk
159 old) were treated with AAV8-Null or AAV8-STAT5$_{CA}$ (0.75 x 10^{11} GC per mouse, iv) and 14 d
160 later livers were collected and used for RNA-seq analysis (see below).
161
162 **AAV8-STAT5$_{CA}$ dose response studies.** Studies to test the ability of AAV-STAT5$_{CA}$ to feminize
163 hepatic gene expression were performed, in compliance with procedures approved by the
164 Boston University Institutional Animal Care and Use Committee (protocol # PROTO201800698),
165 and in compliance with ARRIVE 2.0 Essential 10 guidelines (34), including study design, sample
166 size, randomization, experimental animals and procedures, and statistical methods. Male and
167 female CD1 mice (Crl:CD(ICR), strain code 022), 7-8 wk of age, were purchased from Charles
168 River Laboratories. Mice were housed in a temperature and humidity-controlled environment
169 with a 12-h light, 12-h dark cycle, fed standard rodent chow, and supplied with tap water. AAV8-
170 STAT5$_{CA}$ or AAV8-Luciferase (control) (both produced in-house using methods described
171 below) were administered to male mice by tail vein injection at doses ranging from 0.125 x 10^{11}
172 to 2 x 10^{11} GC per mouse. Virus was diluted into PBS + 35 mM NaCl + 5% glycerol (stabilizer)
173 to give a total injection volume of 150 uL. Mice were euthanized by cervical dislocation at 11 AM
174 (lights on 7:30 AM- 7:30 PM) to minimize the impact of circadian variations of gene expression
175 (35,36).
176
177 **AAV8 production.** AAV coding STAT5b$_{CA}$ and Luciferase (control) was prepared and quantified
178 by triple transfection of HEK293FT cells using methods adapted from protocols provided by
179 Addgene (www.addgene.org). HEK293FT is a fast growing and highly transfectable derivative
180 (cat. #R70007, ThermoFisher Scientific) of the SV40 large T-antigen-expressing HEK293T cell
181 line commonly used for AAV production. On Day 0, 80% confluent flasks of HEK293FT cells
182 were split 1:4 into DMEM culture medium [10% Fetal Bovine Serum (cat. #10437-028, Gibco),
183 1% PenStrep (cat. #15140-122, Gibco)] and then grown overnight to achieve 50-60%
184 confluence at the time of transfection on Day 1. T182.5 flasks were each transfected with a total
185 of 80 µg of plasmid DNA in a 1:1:1 (molar ratio) of three plasmids: pAAV-Helper helper plasmid,
186 which encodes adenovirus genes E2A, E4 and (Cell Biolabs, VA); pAAV2/8 Rep/Cap plasmid
187 (Addgene, plasmid #112864; replication protein derived from AAV-2 serotype, and Capsid
188 protein from AAV-8); and either pENN.AAV.TBG.PI.N-FLAG-tag mSTAT5bCA.WPRE.bGH (see
189 above) or pENN.AAV.TBG.PI.ffLuciferase.RBG (firefly luciferase expressed from TBG promoter;
190 Addgene # 105538). Plasmids were mixed in a 3:1 weight ratio of total plasmid DNA:PEI in 4
191 mL of either OptiMeM™ (Gibco cat. # 31985-062) or serum-free DMEM per flask and then
192 shaken vigorously for 30 sec. The mixture was incubated for 15 min at room temperature in a
193 tissue culture hood, after which 4 ml of the mixture was added to each flask of ~85% confluent
194 HEK293FT cells. After 24 h, the culture medium was replaced by DMEM containing 2% FBS
195 and 1% PenStrep, and the cells were returned to the CO_2 incubator for 5 days.
196
197 Virus was harvested on day 6 after transfection. A cell scraper was used to detach the cells
198 from the flask, followed by collection of the media with cells in sterile 50 mL conical tubes. The
199 tubes were centrifuged at 1000 x g for 10 min at 4°C, and the supernatant was decanted into a
200 sterile bottle. Pellets were pooled and transferred to smaller tubes with 1x PBS + 200 mM NaCl
201 + 0.001% Pluronic F68 (Poloxamer 188 Solution, cat. #P5556-100ML, Sigma) and pelleted
202 again. Cell pellets were frozen at -80 °C for future use in purifying virus. The supernatant (which
203 contains the majority of virus) was filtered through a 0.2 µM PES filter (VWR, cat. #97066-214).

25 mL of 40% PEG8000 (JT Baker, cat. #JTU222-09) was then added for every 100 mL of media supernatant, followed by overnight stirring at 4°C. The next day, the supernatant was incubated for 1 h at 4°C without stirring, to allow for full precipitation of virus before spinning at 2,818 x g for 15 min at 4°C. The supernatant was discarded and the PEG pellet, containing concentrated virus, was resuspended in 10 mL of 1x PBS + 0.001% Pluronic F68 + 200 mM NaCl by pipetting back and forth until the pellet was completely in solution.

The following buffers were prepared for iodixanol purification of the PEG-pelleted virus: (1) 1 M NaCl/PBS-MK Buffer (5.84 g NaCl, 26.3 mg $MgCl_2$ and 14.91 mg KCl dissolved in 1x PBS to give a final volume of 100 mL), sterile filtered through a 0.2 μm PES filter; and (2) 1x PBS-MK Buffer (26.3 mg $MgCl_2$ and 14.91 mg KCl dissolved in 1x PBS to a final volume of 100 mL and then filter-sterilized by passage through a 0.2 μm filter. Iodixanol gradients were prepared as follows: 15% Layer (4.5 mL of 60% Iodixanol (OptiPrep Density Gradient Medium, cat. # D1556-250ML, Sigma) + 13.5 mL of 1M NaCl/PBS-MK Buffer); 25% Layer (5 mL of 60% Iodixanol, 7 mL of 1x PBS-MK Buffer + 30 µL of Phenol Red (cat. #P0290-100ML, Sigma); 40% Layer (6.7 mL of Iodixanol + 3.3 mL of 1x PBS-MK Buffer; 60% layer (10 mL of 60% Iodixanol + 45 µL phenol red). A 10 mL syringe with an 18 g needle and a glass Pasteur pipet were used to layer the Iodixanol gradient in QuickSeal™ tubes (cat. # 344326, Beckman Coulter), from the bottom to the top, starting with 8 mL of the 15% layer, then 6 mL of the 25% layer, 5 mL of the 40% layer and 5 mL of the 60% layer (two tubes per AAV preparation from 10-12 T182.5 flasks). Resuspended virus-PEG pellet solution (5 mL) was added to the top of each gradient and 1x PBS was used to top off each tube before heat sealing. The tubes were spun for 90 min at 350,000 x g in a T70i Rotor at 10°C. The tubes were removed carefully (without disturbing the gradient) and secured to a clamp stand using a clamp. Twenty 1.5 mL Eppendorf tubes were opened and placed in a tube rack beneath the gradient in a biosafety cabinet. The QuickSeal™ tube was punctured at the 40-60% Iodixanol interface with an 18 g needle, using the bevel pointing up, and then the top of the tube was punctured with a 16 g needle. Factions of 1 mL were collected until the 25-45% interface was reached. 5 µL was removed from each fraction for analysis by qPCR to locate AAV-rich fractions before storing the remainder of each fraction at 4°C overnight. Each 5 µL fraction sample was treated with DNase I (cat #M6101, Promega) for 1 h at 37°C and then diluted 1:20 in 50 µg/mL yeast tRNA (cat #AM7119, Invitrogen). A known concentration of plasmid DNA used to prepare the virus was also diluted 1:200 in 50 µg/mL yeast tRNA and processed in parallel. AAV-containing fractions were pooled, typically giving a volume of 4-10 ml.

To concentrate the pooled fractions via buffer exchange, 12 mL of 0.1% Pluronic F68 in 1x PBS was added to a new Amicon Ultra-15 100K Centrifugal Filter Unit (cat. #UFC910024, EMD Millipore) and allowed to incubate at room temperature for 10 min. The Pluronic F68 in PBS was removed from the filtration unit and 12 mL of 0.01% Pluronic F68 in 1x PBS was added to the filtration unit before spinning at 3,000 RPM for 5 min at 4°C. The flow through was discarded and 12 mL of 0.001% Pluronic F68 in 1x PBS + 200 mM NaCl was added and spun at 3000 RPM for 5 min at 4 °C. The flow-through was discarded and up to 12 mL of sample was added to the column and spun at 3500 RPM for 8 min at 4°C. The flow through was discarded and more sample was added up to 12 mL, mixed well with the concentrated remaining sample and spun again. This continued until the sample was concentrated to a total final volume of 0.5-1 mL. The sample was washed with 10 mL of 0.001% Pluronic F68 in 1x PBS + 200 mM NaCl, using a pipette to mix thoroughly, and then spun again. The sample was concentrated to about 0.5 mL, collected using a pipette, and the walls washed with a small volume of 0.001% Pluronic F68 in 1x PBS + 200 mM NaCl to ensure all virus was collected. The concentrated virus was stored at 4°C for up to 2 wk, or at -80°C for long term storage.

255 Using 5 µL of the concentrated virus, purified AAV was treated with DNase I for 30-60 min at
256 37°C to eliminate any contaminating plasmid DNA remaining from the viral purification process.
257 The DNase-treated viral samples were serially diluted 1:20 a total of five times in dilution buffer
258 (50 µg/mL Yeast tRNA, 0.05% Pluronic F68) and the reference plasmid (used to prepare the
259 virus) was serially diluted 1:10 a total of five times in dilution buffer. qPCR was performed as
260 indicated above, using each plasmid dilution series to construct a calibration curve used to
261 determine the titer of the virus.
262
263 **Liver RNA extraction and qPCR analysis.** Total liver RNA was extracted from frozen mouse
264 liver with TRIzol reagent (Invitrogen Life Technologies Inc., Carlsbad, CA), and nuclear RNA
265 was purified from nuclei isolated from frozen liver tissue and then extracted with TRIzol LS as
266 detailed elsewhere (37). RNA (1 µg) was treated with DNase I (cat. #M6101, Promega) to
267 remove DNA contamination. cDNA was then synthesized using High-Capacity cDNA Reverse
268 Transcription Kit (cat. #4368814, Applied Biosystems). qPCR was performed using primers
269 specific to each RNA, designed using Primer Express or Primer3 software
270 (http://bioinfo.ut.ee/primer3-0.4.0/), as follows: Sult3a1: 5'-
271 CATTGTCACATATCCAAAGTCTGGT-3' (forward), 5'-GAAAGGATCTGCTGGGTCCA-3'
272 (reverse) (oligonucleotides# 5735-5736); A1bg: 5'-GAACCCTCTGAGCCCAGTGA-3' (forward),
273 5'- GAGTGGGTGGAGCCTGTGAG-3' (reverse) (oligonucleotides# 5723-5724); Cux2: 5'-
274 CCTCAAGACGAACACCGTCAT-3' (forward), 5'-GCGCATCCTGGACCTGTAGT-3' (reverse)
275 (oligonucleotides# 1382-1383). Quantitative real-time PCR was carried out on a CFX384 Touch
276 Real-Time PCR Detection System (Bio-Rad) using Power SYBR Green PCR Master Mix
277 (ThermoFisher). Normalized linear Ct numbers based on 18S RNA as control were computed to
278 determine the relative expression level of each gene across treatments.
279
280 **RNA-seq analysis.** Polyadenylated mRNA was isolated from 1 µg of total liver RNA or from 1
281 µg of liver nuclear RNA from each treatment group (see below) using NEBNext Poly(A) mRNA
282 Magnetic Isolation Module (cat. #E7490, New England Biolabs). The resulting polyA-selected
283 RNA was used to prepare RNA-seq libraries using the NEBNext Ultra™ Directional RNA Library
284 Prep Kit for Illumina (cat. #E7420L, New England Biolabs), NEBNext Multiplex Oligos for
285 Illumina® Dual Index Primers (cat. #E7600, New England Biolabs), and AMPure XP Beads (cat.
286 #A63881, Beckman Coulter Inc., Indianapolis, IN). RNA-seq libraries were prepared from two
287 independent studies: 1) Sample series #G169: livers from 10-12 wk old male C57Bl/6 mice
288 treated with 0.75 x 10^{11} GC of AAV8-STAT5$_{CA}$ or AAV8-Null control then excised 2 wk later, with
289 two sequencing libraries prepared for each treatment group, each derived from polyA-selected
290 total liver RNA pooled from n = 2 or 3 individual livers (biological replicates); and 2) Sample
291 series #G186: livers from 7-8 wk old male CD1 mice treated with 2 x 10^{11} GC of AAV8-STAT5$_{CA}$
292 or control then excised 4-6 wk later, with a total of 9 sequencing libraries prepared, each one
293 from an individual liver (n=5 AAV8-STAT5$_{CA}$ libraries, n=4 control libraries) and derived from
294 polyA-selected nuclear RNA prepared from nuclei extracted from frozen liver tissue, to increase
295 the sensitivity for detection of the large fraction of lncRNAs that are nuclear-enriched and tightly
296 bound to chromatin in mouse liver (37). Libraries were multiplexed and sequenced by
297 Novogene, Inc (Sacramento, CA) to an average depth of 18-25 million 150 nt paired-end
298 sequence reads on an Illumina HiSeq instrument. RNA-seq data was analyzed using a modified
299 version of the custom pipeline described earlier (15). Briefly, sequence reads were aligned to
300 mouse genome build mm9 (NCBI 37) using STAR aligner (38) and FeatureCounts (39) was
301 used to count sequence reads mapping to the union of the exonic regions in all isoforms of a
302 given gene (collapsed exon counting) based on an mm9 Gene Transfer Format file comprised
303 of 75,798 mouse genes: n = 20,884 RefSeq protein coding genes, n=48,360 mouse liver-
304 expressed lncRNAs genes (a much more complete listing than the set described previously in
305 (40)), n=2,061 RefSeq non-coding genes (NR accession numbers) that do not overlap the set of

306 48,360 lncRNAs, n =4,490 Ensembl non-coding lncRNAs that do not overlap either the RefSeq
307 NR gene set or the 48,360 lncRNA gene set, and n=3 other lncRNAs with interesting liver
308 functions (lnc-LFAR1, LeXis, Lnclgr) (41) and in the gene annotations provided in **Table S1**.
309 Raw sequencing files and processed data files are available at GEO
310 (https://www.ncbi.nlm.nih.gov/geo/) under accession numbers GSE196014 and GSE196015.
311
312 **Differential expression analysis**. EdgeR (42) was used to determine significant differential
313 expression of RNA-seq data for the following comparisons: Males + AAV8-STAT5$_{CA}$ at 2 x 10^{11}
314 GC vs. Control males, and Males + AAV8-STAT5$_{CA}$ at 0.75 x 10^{11} GC vs. AAV8-null males, with
315 full datasets shown in **Tables S1-S3**. Further, a set of 475 sex-biased liver-expressed genes
316 was defined as genes with male liver vs female liver differential expression significant at FDR <
317 0.01 (**Table S2**). A set of 8,246 liver-expressed genes whose differential expression is
318 stringently sex-independent was defined based on |fold-change| for sex-difference < 1.2 and
319 FDR > 0.1 (**Table S3**). All analyses reported here for sex-independent genes used this list of
320 8,246 genes. Finally, for female-biased genes, a percent feminization value was calculated
321 based on each gene's response to each of the following treatments: AAV8-STAT5$_{CA}$ 2 x 10^{11}
322 GC, AAV8-STAT5$_{CA}$ 0.75 x 10^{11} GC, and continuous infusion of male mice with GH (cGH) for 7
323 or 14 d (20), as follows: % feminization = 100% [FPKM (treated male) – FPKM (control
324 male)]/[FPKM (control female) – FPKM (control male)] (**Table S2**).
325
326 Raw RNA-seq data obtained from livers of hypophysectomized mice (15) (GEO accession
327 number GSE66003) was re-analyzed to obtain expression data for the full set of 75,798 mouse
328 genes, including 48,360 liver-expressed lncRNAs, described above. Two distinct classes of sex-
329 biased genes were identified based on differential expression between livers of control and
330 hypophysectomized male and female mice at FDR <0.05 (22): class I male-biased genes are
331 genes that show significantly decreased expression in male liver after hypophysectomy due to
332 their dependence on the male plasma GH pulsatile pattern for expression; and class II male-
333 biased genes are genes that are repressed by the female pituitary profile and, consequently,
334 they are significantly induced in female liver following hypophysectomy. We also identified
335 corresponding sets of class I female-biased genes as those whose expression in female liver
336 decreases significantly after hypophysectomy due to a requirement for the female, near
337 continuous GH pattern for expression, and class II female-biased genes whose expression is
338 repressed by the male pituitary profile and consequently show significant de-repression in
339 hypophysectomized male liver (see Fig. 1 of (43)). The enrichment of STAT5$_{CA}$-responsive
340 genes in each set of hypophysectomy-responsive sex-biased genes was calculated compared
341 to that of a background set of the corresponding class of STAT5$_{CA}$-unresponsive sex-biased
342 genes. Statistical significance was evaluated using Fisher exact test.
343
344 **Enrichment of STAT5 ChIP-seq binding sites at STAT5$_{CA}$-responsive** genes. Male-enriched,
345 female-enriched and sex-independent STAT5 binding sites (1,765, 1,790, and 11,531 sites,
346 respectively) were obtained from our published ChIP-seq data for male and female mouse liver
347 (9) (GEO accession number GSE31578). Each STAT5 binding site was mapped to the closest
348 gene using the command bedtools -closest (44). All genes with a STAT5 binding site within 50
349 kb of the gene body were considered to be a STAT5 target. The enrichment of STAT5$_{CA}$-
350 responsive genes in each set of STAT5 binding site target genes was calculated by comparison
351 to a background set of STAT5$_{CA}$-unresponsive genes. Statistical significance was evaluated
352 using Fisher exact test.
353
354 **Histology.** Fresh liver tissue was submerged into 4% PFA and snap frozen. A portion of each
355 liver was then placed in phosphate-buffered saline with 0.05% NaN_3 for frozen tissue sectioning,
356 and the remainder was transferred to 70% ethanol for paraffin embedding and H&E staining.

Results

Constitutively active STAT5b feminizes liver gene expression. GH-activated JAK2 catalyzes tyrosine phosphorylation linked to the activation and nuclear translocation of STAT5, which enables transcriptional activation of STAT5 target genes. GH-activated liver STAT5 is known to be essential for sex-biased liver gene expression; however, GH also activates other, STAT5-independent signaling pathways (24-26), which could contribute to the regulation of sex-biased gene expression. To determine whether the control of sex-biased liver gene expression by plasma GH pulses (male GH pattern) vs persistent GH stimulation (female GH pattern) is due to the downstream effects of pulsatile vs persistent STAT5 activation *per se*, we expressed a constitutively active form of STAT5 ($STAT5_{CA}$) in male mouse liver to mimic the pattern of persistent STAT5 activation that occurs in female mouse liver (9). $STAT5_{CA}$ cDNA expressed from the hepatocyte-specific thyroxin binding globulin promoter (45,46) was delivered using an AAV serotype 8 vector, which has high intrinsic tropism for the liver (30,31). We validated the AAV8-$STAT5_{CA}$ viral vector by its ability to target STAT5 protein to the nucleus (**Fig. 1A**), which is a key feature of activated STAT5, and by its functional ability to increase hepatic *Igf1* RNA levels and circulating IGF1 in mice deficient in GH receptor signaling in hepatocytes (**Fig. 1B,** aHepGHRkd mouse liver).

Next, we investigated the impact of $STAT5_{CA}$ on sex-biased gene expression in the liver. We delivered AAV8-$STAT5_{CA}$ (2×10^{11} GC/mouse) or a control virus (AAV8-Luciferase) to young adult male mice and excised the livers 4-6 wk later. Liver gene expression was analyzed by nuclear RNA-seq, which enabled us to determine the effects of $STAT5_{CA}$ on the nuclear transcriptome, including lncRNA genes, which are highly enriched in the nucleus owing to their tight binding to chromatin (37) (**Table S1**). AAV8-$STAT5_{CA}$ substantially feminized the expression of liver sex-biased genes. Thus, 154 (59%) of 260 female-biased genes were induced and only 2 female-biased genes were repressed by AAV8-$STAT5_{CA}$ in male liver. Furthermore, 114 (53%) of 215 male-biased genes were repressed and only 5 male-biased genes were induced by AAV8-$STAT5_{CA}$ (**Fig. 2A**, **Table S2**). In contrast, only 1.1% of stringent sex-independent genes (**Table S3**) were induced and 0.7% were repressed by AAV8-$STAT5_{CA}$. These trends, presented for the CD1 mouse liver model used extensively in our studies on liver sex differences (15,19,20,47), were confirmed in an independent study in C57BL6 mice, which were treated with AAV8-$STAT5_{CA}$ at a lower dose and for a shorter duration (0.75×10^{11} GC for 2 wk) (**Fig. 2A,** bottom; **Table S2**). Feminization of the liver transcriptome by AAV8-$STAT5_{CA}$ was dose-dependent, with partial feminization observed at virus doses as low as 0.125×10^{11} GC, as shown for three highly female-biased genes (**Fig. 2B**). Sex-biased genes responsive to AAV8-$STAT5_{CA}$ were enriched for established sex-biased metabolic pathways, whereas the set of sex-independent genes responsive to AAV8-$STAT5_{CA}$ was enriched for extracellular matrix/adhesion and glycoprotein/signal peptide genes (**Fig. 2C, Fig. 2D**).

Role of STAT5 in liver feminization induced by continuous GH infusion (cGH). cGH treatment overrides the endogenous male, pulsatile GH secretion pattern and progressively feminizes liver gene expression over a period of days (20). To understand the role of STAT5 in this process, we compared the changes in gene expression following AAV8-$STAT5_{CA}$ treatment (2×10^{11} GC) to the changes seen in livers of male mice given cGH infusion for 7 or 14 days. AAV8-$STAT5_{CA}$ and cGH infusion induced very similar changes in the expression of sex-biased genes in male liver (**Fig. 3A, Table S2**). Thus, 90% of the female-biased genes induced by AAV8-$STAT5_{CA}$ were also induced by cGH (139/154 genes) and 81% of the male-biased genes repressed by AAV8-$STAT5_{CA}$ were repressed by cGH (92/114 genes) (**Fig. 3B**). Overall, AAV8-$STAT5_{CA}$ and cGH were both highly effective in feminizing liver gene expression, with median feminization values of 87% and 116%, respectively (**Fig. 3C, Table S2**). Female-biased genes

408 that are highly induced (> 100-fold) by cGH infusion or by constitutive activation of STAT5
409 include the cytochrome P450 genes *Cyp3a16, Cyp3a41b, Cyp2c69,* and *Cyp2a4,* and other
410 metabolic genes, such as *Fmo3* and *Hao2.* Of note, 62 female-biased genes were induced in
411 male liver by cGH infusion but not by $STAT5_{CA}$ and 62 male-biased genes were repressed in
412 male liver by cGH infusion but not by $STAT5_{CA}$ (**Fig. 3B, Table S2**). These genes may be
413 regulated by GH signaling pathways independent of STAT5 (25). Finally, four male-biased
414 genes that were repressed by cGH were unexpectedly induced by AAV8-$STAT5_{CA}$ (*Chrna2,*
415 *Fmn2, Nuggc, lnc5159*; **Fig. 3A**, **Table S2**).
416
417 **$STAT5_{CA}$ regulates many direct STAT5 gene targets** - We identified an initial list of potential
418 STAT5 target genes, defined as genes that met the following three criteria: 1) gene expression
419 shows a significant change upon loss of STAT5, as seen in either male or female STAT5-
420 deficient mouse liver (12,19); 2) gene expression is induced or repressed in either male or
421 female liver following pituitary hormone ablation by hypophysectomy, which abolishes GH-
422 dependent STAT5 activation (15); and 3) gene expression is restored when hypophysectomized
423 mice are given an exogenous pulse of GH, which restores pulsatile STAT5 signaling in male
424 liver (15). We filtered out genes showing an inconsistent response to GH treatment or STAT5
425 deficiency to obtain a final list of 227 putative STAT5 target genes, of which 115 showed sex-
426 biased expression (**Table S4**). Importantly, 40% (90 of 227) of the predicted STAT5 target
427 genes and 45% (52 of 115) of the sex-biased predicted STAT5 targets were responsive to
428 AAV8-$STAT5_{CA}$ (**Table S4**, column AC). These $STAT5_{CA}$-responsive STAT5 targets both sex-
429 biased genes and well-established sex-independent STAT5 gene targets, such as *Igf1, Socs2,*
430 *Cish* and *Onecut1*, whose expression was increased in AAV8-$STAT5_{CA}$-treated male mouse
431 liver.
432
433 Next, we investigated whether responsiveness to AAV8-$STAT5_{CA}$ is associated with local
434 STAT5 binding to liver chromatin. We mapped liver STAT5 binding sites identified by chromatin
435 immunoprecipitation (ChIP-seq) (9) to their putative target genes (nearest gene within 50 kb;
436 **Table S2, Table S3**). These sites include many genomic regions where STAT5 binding to liver
437 chromatin is significantly stronger in males than in females, and vice versa (male-enriched and
438 female-enriched STAT5 binding sites, respectively) (9). For each gene class of interest, we
439 determined the enrichment of STAT5 binding in the set of genes responsive to AAV8-$STAT5_{CA}$
440 compared to the set of genes that were unresponsive to AAV8-$STAT5_{CA}$. We observed a strong,
441 significant enrichment of female-biased STAT5 binding at the set of female-biased genes
442 induced by $STAT5_{CA}$ as compared to the corresponding background set of female-biased genes
443 not induced by $STAT5_{CA}$ (**Fig. 4A**, **Table S5**). Male-biased genes repressed by $STAT5_{CA}$ were
444 depleted of STAT5 binding, but not significantly. The strong enrichment of female-biased STAT5
445 binding at female-biased genes induced by $STAT5_{CA}$ indicates that it is the persistence of
446 STAT5 binding, acting in a positive regulatory manner, that induces these female-biased genes
447 in male liver. By contrast, we observed strong enrichment of sex-independent STAT5 binding at
448 sex-independent genes that are repressed by $STAT5_{CA}$, but not at sex-independent genes
449 induced by $STAT5_{CA}$ (**Fig. 4A**). Thus, in the genomic context of these sex-independent genes,
450 STAT5 can act as a repressor, consistent with studies in GH-deficient rat liver (48). Finally, sex-
451 independent genes induced by $STAT5_{CA}$ were enriched for male-biased STAT5 binding,
452 consistent with the positive regulatory potential of those sites evident from our earlier work (9).
453
454 **$STAT5_{CA}$ preferentially induces class I female-biased genes.** In principle, $STAT5_{CA}$ may act
455 by either of two distinct mechanisms. By mimicking the actions of a persistent, female-like
456 plasma GH profile, $STAT5_{CA}$ may induce expression of female-biased genes that are positively
457 regulated by the female GH pattern, i.e., class I female-biased genes. Alternatively, by
458 eliminating the pulsatile nature of STAT5 signaling that is ongoing in male liver (15), $STAT5_{CA}$

459 may effectively override the inhibitory activity that endogenous male plasma GH pulses exert on
460 class II female-biased genes and thereby de-repress their expression (22). To distinguish these
461 two models, we compared the hypophysectomy response class frequency of the female-biased
462 genes that are induced by $STAT5_{CA}$ to those that are not induced by $STAT5_{CA}$ (**Table S2**, **Table**
463 **S5**). We found that the set of $STAT5_{CA}$-induced female-biased genes is significantly enriched in
464 class I female-biased genes; furthermore, it is significantly depleted of class II female-biased
465 genes (**Fig. 4B**, left). No significant hypophysectomy class enrichment was seen for $STAT5_{CA}$-
466 repressed male-biased genes. Sex-independent genes induced by $STAT5_{CA}$ showed a highly
467 significant 7-fold depletion of genes whose expression was induced when GH was ablated by
468 hypophysectomy, whereas sex-independent genes repressed by $STAT5_{CA}$ showed a tendency
469 toward enrichment for genes induced by hypophysectomy (**Fig. 4B,** right), both consistent with
470 the GH mimic nature of $STAT5_{CA}$.
471
472 **Dose-dependent effects of AAV8-$STAT5_{CA}$ on liver histology and *Igf1* expression.** There
473 were no consistent changes in hepatocyte morphology when AAV8-$STAT5_{CA}$ was delivered at
474 doses up to 0.75 x 10^{11} GC or in livers from mice given cGH infusion. However, when the dose
475 of AAV8-$STAT5_{CA}$ was increased to 2 x 10^{11} GC/mouse, we observed architectural distortion,
476 hepatocyte hyperplasia, binuclear hepatocytes, karyomegaly and nuclear atypia (**Fig. 5**). To
477 ascertain whether these responses are associated with STAT5 overexpression, we examined
478 the expression levels of two classical STAT target genes in liver, *Igf1* and *Socs2.* Whereas
479 AAV8-$STAT5_{CA}$ induced the expression of *Igf1* moderately (2-2.5-fold increase above control
480 liver levels at both doses), we observed strong induction of *Socs2,* which reached 8.5-fold at the
481 lower dose and 14.4-fold above baseline at the higher dose (2 x 10^{11} GC), consistent with a
482 functional overexpression of STAT5 activity at the higher AAV8-$STAT5_{CA}$ dose (**Fig. 6**).
483
484 **Discussion**
485
486 The sex-dependent patterns of pituitary GH secretion – pulsatile GH release in males and
487 persistent (near-continuous) GH release in females – activate hepatic GH receptor signaling to
488 STAT5 in a manner that mirrors circulating GH profiles, i.e., pulsatile STAT5 activation and
489 transcriptional activity in male liver, and persistent STAT5 activation in female liver. Here we
490 show that persistent expression of activated STAT5, achieved using a liver-specific AAV8 viral
491 vector to deliver the activated STAT5b mutant $STAT5_{CA}$ to mouse hepatocytes *in vivo*, has
492 extensive effects on sex-biased gene expression in the liver, with large numbers of male-biased
493 genes repressed and female-biased genes induced. These effects are highly selective for sex-
494 biased genes, insofar as fewer than 2% of genes showing sex-independent expression were
495 impacted by $STAT5_{CA}$ delivery. Many of the sex-independent gene responses are likely to be
496 specific, in view of their enrichment for specific biological pathways related to extracellular
497 matrix/cell adhesion and Wnt signaling.
498
499 Continuous infusion of GH in male mice (cGH treatment) mimics the endogenous female pattern
500 of persistent circulating GH and overrides the endogenous pulsatile male secretion pattern,
501 leading to substantial feminization of liver gene expression within 7 days (20,21). Here, we
502 report a high overlap between gene responses to $STAT5_{CA}$ expression and cGH infusion,
503 providing strong evidence that persistent STAT5 activity alone is sufficient to account for a large
504 fraction of the feminized genes. Nevertheless, some genes responded in a unique manner to
505 either $STAT5_{CA}$ expression or cGH infusion. While some of the differences in response to these
506 two feminizing treatments may be due to cutoff thresholds, others clearly are not, for example
507 *Cyp2b10* and *Cyp2c37*, whose expression in male liver was induced, and substantially
508 feminized, by cGH infusion but which were unresponsive to $STAT5_{CA}$ (**Table S2**). Differences
509 between these two models for feminizing male liver gene expression may in part be due to

510 STAT5-independent signaling pathways that are initiated by continuous GH, such as the GH
511 receptor-dependent activation of PI-3 kinase, ERK signaling and Src family kinases (25).
512
513 $STAT5_{CA}$ and cGH infusion both increased the expression of some female-biased genes to a
514 level that exceeds levels of expression seen in untreated female liver. This phenomenon was
515 somewhat more pronounced with cGH infusion (29 genes expressed at >2-fold the level of
516 female liver after 14 days of cGH infusion vs. 18 genes exceeded that level following $STAT5_{CA}$
517 treatment; **Table S2**). There are several possible reasons for the excessive feminization
518 observed for these genes, and for the incomplete feminization observed for many other sex-
519 biased genes. First, levels of STAT5 activity reached in AAV8-$STAT5_{CA}$-infected hepatocytes
520 may exceed the physiological levels of activated STAT5 in female liver, in particular at the
521 higher dose of AAV8-$STAT5_{CA}$ used in our study (c.f., overexpression of *Socs2*; **Fig. 6**). Related
522 to this, both treatments used in this study, cGH infusion and expression of a persistently
523 activated STAT5, differ somewhat from the physiological patterns in female liver, where there
524 are short GH-off time periods, albeit not as prolonged or as frequent as the GH-off inter-pulse
525 intervals that characterize males. Second, although $STAT5_{CA}$ and cGH may both mimic female
526 liver with respect to STAT5 activity and GH stimulation, they do not recapitulate the female
527 hormonal environment with respect to other factors. One such factor is estrogen, which can also
528 impact sex-biased gene expression in the liver, albeit it affects only 4% of liver sex-biased
529 genes in a direct estrogen receptor-dependent manner (49). Indeed, it is remarkable how
530 effective $STAT5_{CA}$ and cGH are in feminizing male liver, despite the presence of a male gonadal
531 steroid environment. Finally, intrinsic chromosomal sex differences associated with liver-
532 expressed Y-chromosome-encoded epigenetic modifiers, such as *Uty* and *Kdm5d,* and partial
533 X-inactivation/incomplete gene dosage compensation remain (50) and could also contribute to
534 the observed differences between female liver and $STAT5_{CA}$-treated or cGH-infused male liver.
535
536 Female-biased genes induced by $STAT5_{CA}$ in male liver were significantly enriched for nearby
537 female-biased STAT5 binding sites in liver chromatin when compared to the set of female-
538 biased genes that were not induced by $STAT5_{CA}$. Moreover, the $STAT5_{CA}$-induced female-
539 biased genes were significantly enriched for class I female-biased genes, whose expression in
540 female liver is positively regulated by the female plasma GH pattern. Together, these findings
541 lend strong support to the proposal that the de-repression of these female-biased genes in male
542 liver involves direct binding of $STAT5_{CA}$ to these STAT5-binding regulatory sites in association
543 with induction of local, female-biased chromatin opening, which has been linked to female-
544 biased STAT5 binding and gene activation (9,17). Female-biased genes not induced by
545 $STAT5_{CA}$ could be regulated by other mechanisms, including GH signaling independent of
546 STAT5, as noted above. We did not observe a corresponding enrichment of STAT5 binding
547 sites nearby male-biased genes repressed by $STAT5_{CA}$, indicating that factors other than
548 differences in STAT5 binding determine whether an individual male-biased gene will be
549 repressed by $STAT5_{CA}$ expression in male liver. Finally, sex-independent genes repressed by
550 $STAT5_{CA}$ showed strong enrichment for local sex-independent STAT5 binding sites, supporting
551 the proposal that STAT5 can repress gene expression by a direct DNA binding mechanism.
552
553 We observed significant feminization of gene expression at AAV8-$STAT5_{CA}$ doses as low as
554 0.125×10^{11} GC per mouse, i.e., 10-fold or more lower than standard doses of 2×10^{11}
555 commonly used for AAV8-induced gene expression in mouse liver (31). This finding is in line
556 with earlier studies in a GH-deficient rat model, where infusion of GH at a dose that results in as
557 low as 3% of the nominal circulating female GH level restores the expression of certain female-
558 biased genes, while other genes require higher GH doses and show only partial induction (51).
559

560 It is well established that a reduction of GH signaling is associated with liver steatosis and
561 development of non-alcoholic steatohepatitis, both in humans and in mouse models, and
562 increasing GH signaling can improve fatty liver endpoints (52,53). However, we found that
563 treatment with a high dose of AAV8-STAT5$_{CA}$ resulted in certain histopathological changes
564 indicative of liver injury that cannot be attributed to the AAV8 infection *per se*, as they were not
565 seen in AAV-Luciferase controls. Livers from mice given cGH infusion for 17 days did not show
566 corresponding histopathological changes, despite the overall similarity of its effects on sex-
567 biased gene expression. Conceivably, the histopathology associated with AAV8-STAT5$_{CA}$ at the
568 high dose could be related to the propensity of this viral vector to integrate into the host genome
569 in the context of liver injury (54,55) or could be a supraphysiologic effect of STAT5
570 overexpression. Nonetheless, these observations highlight the importance of carefully
571 evaluating such effects before considering STAT5$_{CA}$ or other STAT5 derivatives for therapeutic
572 use in treating liver disease.
573
574 **Acknowledgements** – The authors thank the following Waxman lab members: Kritika Karri for
575 providing annotations for the 48,360 mouse liver-expressed lncRNAs genes examined in this
576 study, Dr. Maxim Pyatkov for RNA-seq analysis pipeline development, and Dr. Ravi Sonkar for
577 assistance with histology imaging.
578
579 **Data availability.** All data generated or analyzed during this study are included in this published
580 article or in the associated Supplemental tables and the public data repository at GEO
581 (https://www.ncbi.nlm.nih.gov/geo/) under accession numbers GSE196014 and GSE196015.
582
583
584 **References**
585
586 1. Waxman DJ, Holloway MG. Sex differences in the expression of hepatic drug metabolizing
587 enzymes. *Mol Pharmacol*. 2009;76(2):215-228.

588 2. Kur P, Kolasa-Wolosiuk A, Misiakiewicz-Has K, Wiszniewska B. Sex Hormone-Dependent
589 Physiology and Diseases of Liver. *Int J Environ Res Public Health*. 2020;17(8).

590 3. Lonardo A, Nascimbeni F, Ballestri S, Fairweather D, Win S, Than TA, Abdelmalek MF, Suzuki
591 A. Sex Differences in Nonalcoholic Fatty Liver Disease: State of the Art and Identification of
592 Research Gaps. *Hepatology*. 2019;70(4):1457-1469.

593 4. Brie B, Ramirez MC, De Winne C, Lopez Vicchi F, Villarruel L, Sorianello E, Catalano P,
594 Ornstein AM, Becu-Villalobos D. Brain Control of Sexually Dimorphic Liver Function and
595 Disease: The Endocrine Connection. *Cell Mol Neurobiol*. 2019;39(2):169-180.

596 5. Waxman DJ, Pampori NA, Ram PA, Agrawal AK, Shapiro BH. Interpulse interval in circulating
597 growth hormone patterns regulates sexually dimorphic expression of hepatic cytochrome
598 P450. *Proc Natl Acad Sci U S A*. 1991;88(15):6868-6872.

599 6. Mode A, Wiersma-Larsson E, Strom A, Zaphiropoulos PG, Gustafsson JA. A dual role of
600 growth hormone as a feminizing and masculinizing factor in the control of sex-specific
601 cytochrome P-450 isozymes in rat liver. *J Endocrinol*. 1989;120(2):311-317.

602 7. Waters MJ. The growth hormone receptor. *Growth Horm IGF Res*. 2016;28:6-10.

603 8. Piwien-Pilipuk G, Huo JS, Schwartz J. Growth hormone signal transduction. *J Pediatr*
604 *Endocrinol Metab*. 2002;15(6):771-786.

605 9. Zhang Y, Laz EV, Waxman DJ. Dynamic, sex-differential STAT5 and BCL6 binding to sex-
606 biased, growth hormone-regulated genes in adult mouse liver. *Mol Cell Biol*. 2012;32(4):880-
607 896.

608 10. Chia DJ. Minireview: mechanisms of growth hormone-mediated gene regulation. *Mol*
609 *Endocrinol*. 2014;28(7):1012-1025.

610 11. Clodfelter KH, Holloway MG, Hodor P, Park SH, Ray WJ, Waxman DJ. Sex-dependent liver
611 gene expression is extensive and largely dependent upon signal transducer and activator of
612 transcription 5b (STAT5b): STAT5b-dependent activation of male genes and repression of
613 female genes revealed by microarray analysis. *Mol Endocrinol*. 2006;20(6):1333-1351.

614 12. Holloway MG, Cui Y, Laz EV, Hosui A, Hennighausen L, Waxman DJ. Loss of sexually
615 dimorphic liver gene expression upon hepatocyte-specific deletion of Stat5a-Stat5b locus.
616 *Endocrinology*. 2007;148(5):1977-1986.

617 13. Choi HK, Waxman DJ. Plasma growth hormone pulse activation of hepatic JAK-STAT5
618 signaling: developmental regulation and role in male-specific liver gene expression.
619 *Endocrinology*. 2000;141(9):3245-3255.

620 14. Tannenbaum GS, Choi HK, Gurd W, Waxman DJ. Temporal relationship between the sexually
621 dimorphic spontaneous GH secretory profiles and hepatic STAT5 activity. *Endocrinology*.
622 2001;142(11):4599-4606.

623 15. Connerney J, Lau-Corona D, Rampersaud A, Waxman DJ. Activation of Male Liver Chromatin
624 Accessibility and STAT5-Dependent Gene Transcription by Plasma Growth Hormone Pulses.
625 *Endocrinology*. 2017;158(5):1386-1405.

626 16. Choi HK, Waxman DJ. Growth hormone, but not prolactin, maintains, low-level activation of
627 STAT5a and STAT5b in female rat liver. *Endocrinology*. 1999;140(11):5126-5135.

628 17. Sugathan A, Waxman DJ. Genome-wide analysis of chromatin states reveals distinct
629 mechanisms of sex-dependent gene regulation in male and female mouse liver. *Mol Cell Biol*.
630 2013;33(18):3594-3610.

631 18. Cui Y, Hosui A, Sun R, Shen K, Gavrilova O, Chen W, Cam MC, Gao B, Robinson GW,
632 Hennighausen L. Loss of signal transducer and activator of transcription 5 leads to
633 hepatosteatosis and impaired liver regeneration. *Hepatology*. 2007;46(2):504-513.

634 19. Hao P, Waxman DJ. STAT5 Regulation of Sex-Dependent Hepatic CpG Methylation at Distal
635 Regulatory Elements Mapping to Sex-Biased Genes. *Mol Cell Biol*. 2021;41(2).

636 20. Lau-Corona D, Suvorov A, Waxman DJ. Feminization of Male Mouse Liver by Persistent
637 Growth Hormone Stimulation: Activation of Sex-Biased Transcriptional Networks and
638 Dynamic Changes in Chromatin States. *Mol Cell Biol*. 2017;37(19).

639 21. Holloway MG, Laz EV, Waxman DJ. Codependence of growth hormone-responsive, sexually
640 dimorphic hepatic gene expression on signal transducer and activator of transcription 5b and
641 hepatic nuclear factor 4alpha. *Mol Endocrinol*. 2006;20(3):647-660.

642 22. Wauthier V, Sugathan A, Meyer RD, Dombkowski AA, Waxman DJ. Intrinsic sex differences
643 in the early growth hormone responsiveness of sex-specific genes in mouse liver. *Mol*
644 *Endocrinol*. 2010;24(3):667-678.

645 23. Rotwein P. Regulation of gene expression by growth hormone. *Mol Cell Endocrinol*.
646 2020;507:110788.

647 24. Chhabra Y, Lee CMM, Muller AF, Brooks AJ. GHR signalling: Receptor activation and
648 degradation mechanisms. *Mol Cell Endocrinol*. 2021;520:111075.

649 25. Frank SJ. Classical and novel GH receptor signaling pathways. *Mol Cell Endocrinol*.
650 2020;518:110999.

651 26. Carter-Su C, Schwartz J, Argetsinger LS. Growth hormone signaling pathways. *Growth Horm*
652 *IGF Res*. 2016;28:11-15.

653 27. List EO, Berryman DE, Funk K, Jara A, Kelder B, Wang F, Stout MB, Zhi X, Sun L, White TA,
654 LeBrasseur NK, Pirtskhalava T, Tchkonia T, Jensen EA, Zhang W, Masternak MM, Kirkland
655 JL, Miller RA, Bartke A, Kopchick JJ. Liver-specific GH receptor gene-disrupted (LiGHRKO)
656 mice have decreased endocrine IGF-I, increased local IGF-I, and altered body size, body
657 composition, and adipokine profiles. *Endocrinology*. 2014;155(5):1793-1805.

658 28. Ariyoshi K, Nosaka T, Yamada K, Onishi M, Oka Y, Miyajima A, Kitamura T. Constitutive
659 activation of STAT5 by a point mutation in the SH2 domain. *J Biol Chem*. 2000;275(32):24407-
660 24413.

661 29. Woelfle J, Billiard J, Rotwein P. Acute control of insulin-like growth factor-I gene transcription
662 by growth hormone through Stat5b. *J Biol Chem*. 2003;278(25):22696-22702.

663 30. Zincarelli C, Soltys S, Rengo G, Rabinowitz JE. Analysis of AAV serotypes 1-9 mediated gene
664 expression and tropism in mice after systemic injection. *Mol Ther*. 2008;16(6):1073-1080.

665 31. Sands MS. AAV-mediated liver-directed gene therapy. *Methods Mol Biol*. 2011;807:141-157.

666 32. List EO, Berryman DE, Funk K, Gosney ES, Jara A, Kelder B, Wang X, Kutz L, Troike K,
667 Lozier N, Mikula V, Lubbers ER, Zhang H, Vesel C, Junnila RK, Frank SJ, Masternak MM,
668 Bartke A, Kopchick JJ. The role of GH in adipose tissue: lessons from adipose-specific GH
669 receptor gene-disrupted mice. *Mol Endocrinol*. 2013;27(3):524-535.

670 33. Cordoba-Chacon J, Majumdar N, List EO, Diaz-Ruiz A, Frank SJ, Manzano A, Bartrons R,
671 Puchowicz M, Kopchick JJ, Kineman RD. Growth Hormone Inhibits Hepatic De Novo
672 Lipogenesis in Adult Mice. *Diabetes*. 2015;64(9):3093-3103.

673 34. Percie du Sert N, Ahluwalia A, Alam S, Avey MT, Baker M, Browne WJ, Clark A, Cuthill IC,
674 Dirnagl U, Emerson M, Garner P, Holgate ST, Howells DW, Hurst V, Karp NA, Lazic SE,
675 Lidster K, MacCallum CJ, Macleod M, Pearl EJ, Petersen OH, Rawle F, Reynolds P, Rooney

676 K, Sena ES, Silberberg SD, Steckler T, Würbel H. Reporting animal research: Explanation
677 and elaboration for the ARRIVE guidelines 2.0. *PLoS Biol*. 2020;18(7):e3000411.

678 35. Wang J, Symul L, Yeung J, Gobet C, Sobel J, Luck S, Westermark PO, Molina N, Naef F.
679 Circadian clock-dependent and -independent posttranscriptional regulation underlies
680 temporal mRNA accumulation in mouse liver. *Proc Natl Acad Sci U S A*. 2018;115(8):E1916-
681 E1925.

682 36. Menet JS, Rodriguez J, Abruzzi KC, Rosbash M. Nascent-Seq reveals novel features of
683 mouse circadian transcriptional regulation. *Elife*. 2012;1:e00011.

684 37. Goldfarb CN, Waxman DJ. Global analysis of expression, maturation and subcellular
685 localization of mouse liver transcriptome identifies novel sex-biased and TCPOBOP-
686 responsive long non-coding RNAs. *BMC Genomics*. 2021;22(1):212.

687 38. Dobin A, Davis CA, Schlesinger F, Drenkow J, Zaleski C, Jha S, Batut P, Chaisson M,
688 Gingeras TR. STAR: ultrafast universal RNA-seq aligner. *Bioinformatics*. 2013;29(1):15-21.

689 39. Liao Y, Smyth GK, Shi W. featureCounts: an efficient general purpose program for assigning
690 sequence reads to genomic features. *Bioinformatics*. 2014;30(7):923-930.

691 40. Lodato NJ, Melia T, Rampersaud A, Waxman DJ. Sex-Differential Responses of Tumor
692 Promotion-Associated Genes and Dysregulation of Novel Long Noncoding RNAs in
693 Constitutive Androstane Receptor-Activated Mouse Liver. *Toxicol Sci*. 2017;159(1):25-41.

694 41. Goldfarb CN, Karri K, Pyatkov M, Waxman DJ. Interplay between murine sex-biased gene
695 expression and hepatic zonation revealed by single nucleus RNA sequencing. *bioRxiv*.
696 2022:2022.2001.2018.476791.

697 42. Robinson MD, McCarthy DJ, Smyth GK. edgeR: a Bioconductor package for differential
698 expression analysis of digital gene expression data. *Bioinformatics*. 2010;26(1):139-140.

699 43. Melia T, Waxman DJ. Sex-Biased lncRNAs Inversely Correlate With Sex-Opposite Gene
700 Coexpression Networks in Diversity Outbred Mouse Liver. *Endocrinology*. 2019;160(5):989-
701 1007.

702 44. Quinlan AR, Hall IM. BEDTools: a flexible suite of utilities for comparing genomic features.
703 *Bioinformatics*. 2010;26(6):841-842.

704 45. Kiourtis C, Wilczynska A, Nixon C, Clark W, May S, Bird TG. Specificity and off-target effects
705 of AAV8-TBG viral vectors for the manipulation of hepatocellular gene expression in mice.
706 *Biol Open*. 2021;10(9).

707 46. Wolf Greenstein A, Majumdar N, Yang P, Subbaiah PV, Kineman RD, Cordoba-Chacon J.
708 Hepatocyte-specific, PPARgamma-regulated mechanisms to promote steatosis in adult mice.
709 *J Endocrinol*. 2017;232(1):107-121.

710 47. Melia T, Hao P, Yilmaz F, Waxman DJ. Hepatic Long Intergenic Noncoding RNAs: High
711 Promoter Conservation and Dynamic, Sex-Dependent Transcriptional Regulation by Growth
712 Hormone. *Mol Cell Biol*. 2016;36(1):50-69.

713 48. Ono M, Chia DJ, Merino-Martinez R, Flores-Morales A, Unterman TG, Rotwein P. Signal
714 transducer and activator of transcription (Stat) 5b-mediated inhibition of insulin-like growth
715 factor binding protein-1 gene transcription: a mechanism for repression of gene expression
716 by growth hormone. *Mol Endocrinol*. 2007;21(6):1443-1457.

717 49. Zheng D, Wang X, Antonson P, Gustafsson JA, Li Z. Genomics of sex hormone receptor
718 signaling in hepatic sexual dimorphism. *Mol Cell Endocrinol*. 2018;471:33-41.

719 50. Naqvi S, Godfrey AK, Hughes JF, Goodheart ML, Mitchell RN, Page DC. Conservation,
720 acquisition, and functional impact of sex-biased gene expression in mammals. *Science*.
721 2019;365(6450).

722 51. Pampori NA, Shapiro BH. Gender differences in the responsiveness of the sex-dependent
723 isoforms of hepatic P450 to the feminine plasma growth hormone profile. *Endocrinology*.
724 1999;140(3):1245-1254.

725 52. Vazquez-Borrego MC, Del Rio-Moreno M, Kineman RD. Towards Understanding the Direct
726 and Indirect Actions of Growth Hormone in Controlling Hepatocyte Carbohydrate and Lipid
727 Metabolism. *Cells*. 2021;10(10).

728 53. Kaltenecker D, Themanns M, Mueller KM, Spirk K, Suske T, Merkel O, Kenner L, Luis A,
729 Kozlov A, Haybaeck J, Muller M, Han X, Moriggl R. Hepatic growth hormone - JAK2 - STAT5
730 signalling: Metabolic function, non-alcoholic fatty liver disease and hepatocellular carcinoma
731 progression. *Cytokine*. 2019;124:154569.

732 54. Dalwadi DA, Torrens L, Abril-Fornaguera J, Pinyol R, Willoughby C, Posey J, Llovet JM,
733 Lanciault C, Russell DW, Grompe M, Naugler WE. Liver Injury Increases the Incidence of
734 HCC following AAV Gene Therapy in Mice. *Mol Ther*. 2021;29(2):680-690.

735 55. Deyle DR, Russell DW. Adeno-associated virus vector integration. *Curr Opin Mol Ther*.
736 2009;11(4):442-447.
737
738

Figure legends

Fig. 1. Functional validation of AAV8-STAT5$_{CA}$ *in vivo*. (A) Nuclear localization of Flag-Tag STAT5$_{CA}$ protein, detected by anti-Flag antibody on a Western blot of nuclear extracts from livers excised from mice 7 d after injection of AAV8-Null (control, lanes 1, 3) or AAV8-STAT5$_{CA}$ (1.5 x 10^{11} GC, lanes 2, 4). Extracts were prepared from four individual livers. (B) Plasma IGF1 levels and liver Igf1 and GH receptor (Ghr) mRNA levels in male mice, GH receptor floxed control (Null) male mice, or male mice with adult-onset GH receptor knockdown (aHepGHRkd mice), with or without AAV8-STAT5$_{CA}$ treatment at the doses indicated. Values shown are mean ± SEM for n = 8 mice per group. Significance was evaluated by one way ANOVA with Bonferroni multiple comparison correction, implemented in GraphPad Prism. For comparisons to aHepGHRkd (second bar in each set): p< 0.001, ***; p< 0.01, **; and p=0.0595, *. NS, p > 0.05 for comparisons to Null, indicating restoration of Igf1 RNA and plasma protein.

Fig. 2. **AAV8-STAT5$_{CA}$ responsive genes in male liver**. (A) Percentage of all genes that are either consistently sex biased at FDR < 0.05 (Table S2, n= 475 genes) or stringently sex-independent (SI) genes (Table S3, n = 8,246 genes) and whose expression in AAV8-STAT5$_{CA}$-treated liver (as indicated) is significantly induced or repressed compared to control liver (FDR < 0.05). Top panel: results for CD-1 male mice; bottom panel: results for C57BL/6 mice. GC, genome copies of AAV8 virus. Number of responding genes is shown above each bar. (B) Dose responses for AAV8-STAT5$_{CA}$ induction of three highly female-biased genes. Data based on RT-qPCR analysis of liver RNA, mean +/- SEM for n=2-6 livers per group, expressed as percentage of gene expression in control (untreated) female (F) mouse liver. M, male group. (C, D) DAVID pathway analysis of the sets of sex-biased genes (C) and sex-independent genes (D) that are responsive to STAT5$_{CA}$. Shown are the top five enriched clusters, with bars indicating -log10 P values (Benjamini-Hochberg corrected) for enrichment.

Fig. 3. **Effects of STAT5$_{CA}$ and cGH infusion on sex-biased gene expression**. (A) Heatmap showing impact of STAT5$_{CA}$ or cGH infusion on the expression of 275 responsive sex-biased genes (log2 Fold-change increases (red) or decreases (blue)) in male mouse liver. M, male; F, female. (B) Overlap between female-biased genes induced by AAV8-STAT5$_{CA}$ and those induced by cGH after either 7 or 14 days (left), and between male-biased genes repressed by AAV8-STAT5$_{CA}$ and those repressed by cGH after either 7 or 14 days (right). Excluded are 5 male-biased genes induced by AAV8-STAT5$_{CA}$ and 1 female-biased genes repressed by AAV8-STAT5$_{CA}$. (C) Boxplots showing the distribution of feminization values for 139 female-biased genes induced in male liver in both mouse models (see Table S2). Median value, horizontal line in each box.

Fig. 4. Enrichment of STAT5 binding sites (A) and hypophysectomy response class (B) for the sets of genes induced or repressed by STAT5$_{CA}$. (A) Data are shown for STAT5 binding sites that are male-biased (M; 1,765 sites), female-biased (F; 1,790 sites), and sex-independent (SI; 11,531 sites), as defined by ChIP-seq, and mapped to their target genes (nearest gene within 50 kb). Enrichments are expressed as the ratio of STAT5$_{CA}$-responsive genes compared to STAT5$_{CA}$-unresponsive genes that are associated with each of the 3 sets of STAT5 binding sites. (B) Enrichment of class I or class II sex-biased genes (left) and sex-independent genes (right) in the STAT5$_{CA}$-responsive gene sets, expressed as the ratio of the number of STAT5$_{CA}$-responsive genes compared to the number of STAT5$_{CA}$-unresponsive genes in each class (left) or that are induced or repressed by hypophysectomy (right). Significance was determined by Fishers exact test: *, p< 0.05, ***, P < 0.001. Blue asterisks, significant enrichment; red asterisks, significant depletion.

790 **Fig. 5**. **H&E staining of AAV8-STAT5$_{CA}$-infected liver**. Liver sections from mice treated with
791 AAV8-STAT5$_{CA}$ or AAV8-Luciferase at the indicated GC dose per mouse were stained with
792 H&E, revealing a STAT5$_{CA}$ dose-dependent histopathology, which was evident and most
793 consistent at the highest dose of AAV8 dose. No histopathology was evident in mice given cGH
794 infusion for 17 days. Images collected with an Olympus FSX-100 instrument at 16x.
795
796 **Fig. 6**. Expression of direct STAT5 target genes *Igf1* and *Socs2* in male liver: impact of cGH
797 infusion and AAV8-STAT5$_{CA}$. Shown are expression level determined by RNA-seq (fold-change
798 values relative to male control), indicating supraphysiological induction of *Socs2*, and to a lesser
799 extent *Igf1*, by AAV8-STAT5$_{CA.}$ Significance was determined by edgeR: ***, adjusted p-value <
800 E-05.
801

Fig. 1

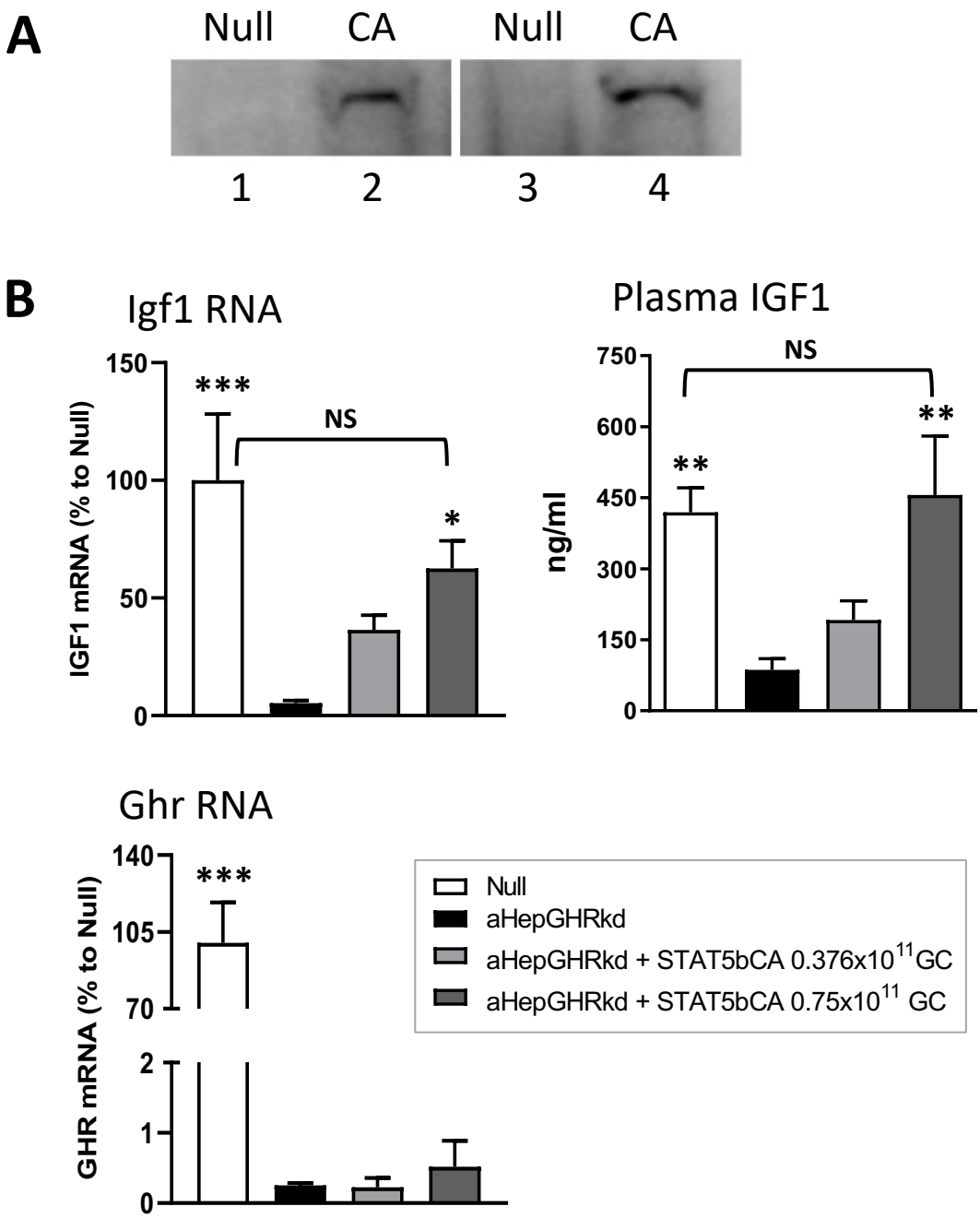
A
Null
CA
Null
CA
1
2
3
4
B
Igf1 RNA
IGF1 mRNA (% to Null)
150
100
50
0
***
NS
*
Plasma IGF1
ng/ml
750
600
450
300
150
0
NS
**
**
Ghr RNA
GHR mRNA (% to Null)
140
105
70
2
1
0
***
Null
aHepGHRkd
aHepGHRkd + STAT5bCA 0.376x10^11GC
aHepGHRkd + STAT5bCA 0.75x10^11 GC

Fig. 2

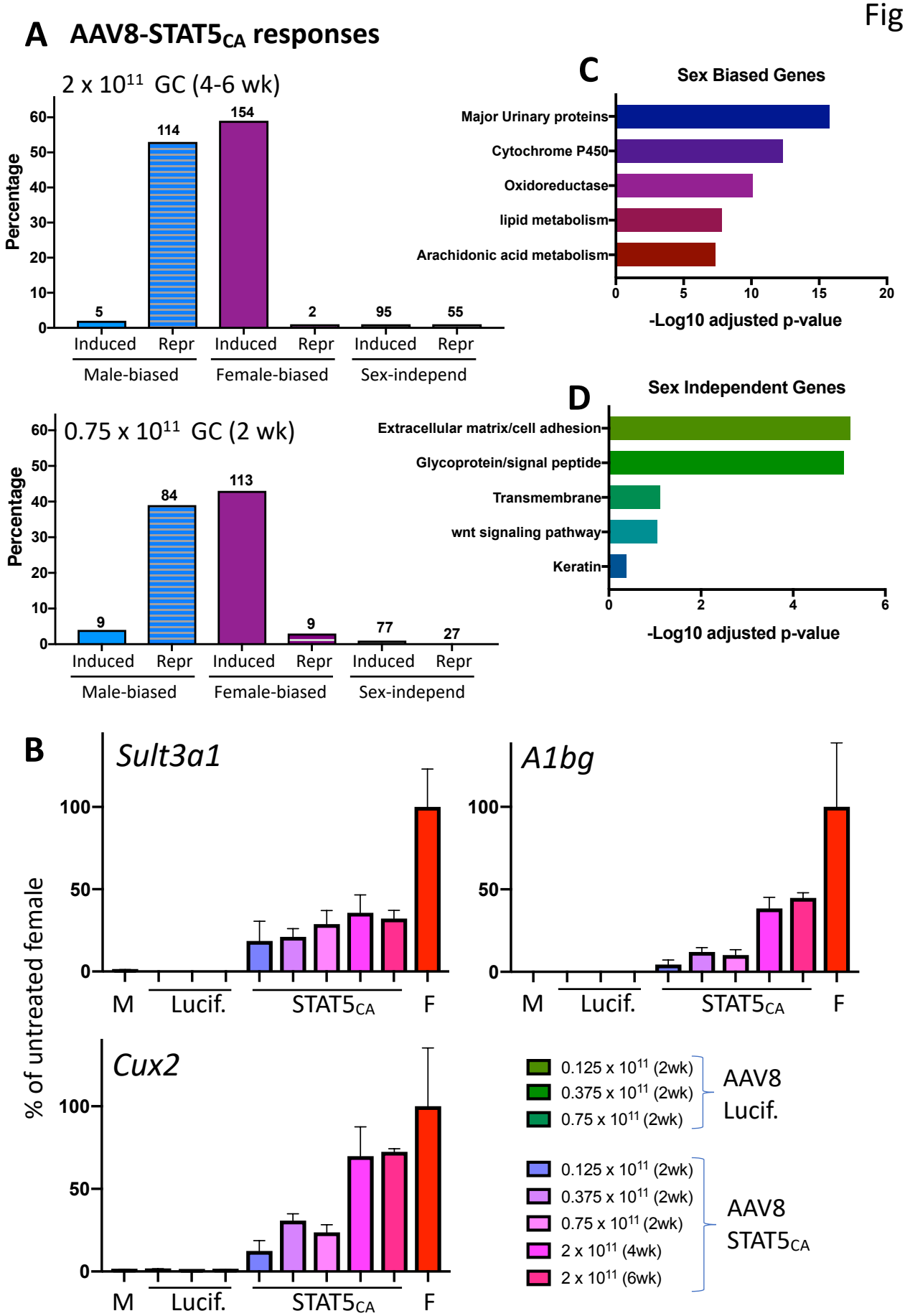
A
AAV8-STAT5CA responses
2 x 10^11 GC (4-6 wk)
Percentage
60
50
40
30
20
10
0
5
114
154
2
95
55
Induced
Repr
Induced
Repr
Induced
Repr
Male-biased
Female-biased
Sex-independ
0.75 x 10^11 GC (2 wk)
Percentage
60
50
40
30
20
10
0
9
84
113
9
77
27
Induced
Repr
Induced
Repr
Induced
Repr
Male-biased
Female-biased
Sex-independ
C
Sex Biased Genes
Major Urinary proteins
Cytochrome P450
Oxidoreductase
lipid metabolism
Arachidonic acid metabolism
0
5
10
15
20
-Log10 adjusted p-value
D
Sex Independent Genes
Extracellular matrix/cell adhesion
Glycoprotein/signal peptide
Transmembrane
wnt signaling pathway
Keratin
0
2
4
6
-Log10 adjusted p-value
B
Sult3a1
A1bg
Cux2
% of untreated female
100
50
0
M
Lucif.
STAT5CA
F
0.125 x 10^11 (2wk)
0.375 x 10^11 (2wk)
0.75 x 10^11 (2wk)
AAV8
Lucif.
0.125 x 10^11 (2wk)
0.375 x 10^11 (2wk)
0.75 x 10^11 (2wk)
2 x 10^11 (4wk)
2 x 10^11 (6wk)
AAV8
STAT5CA

Fig. 3

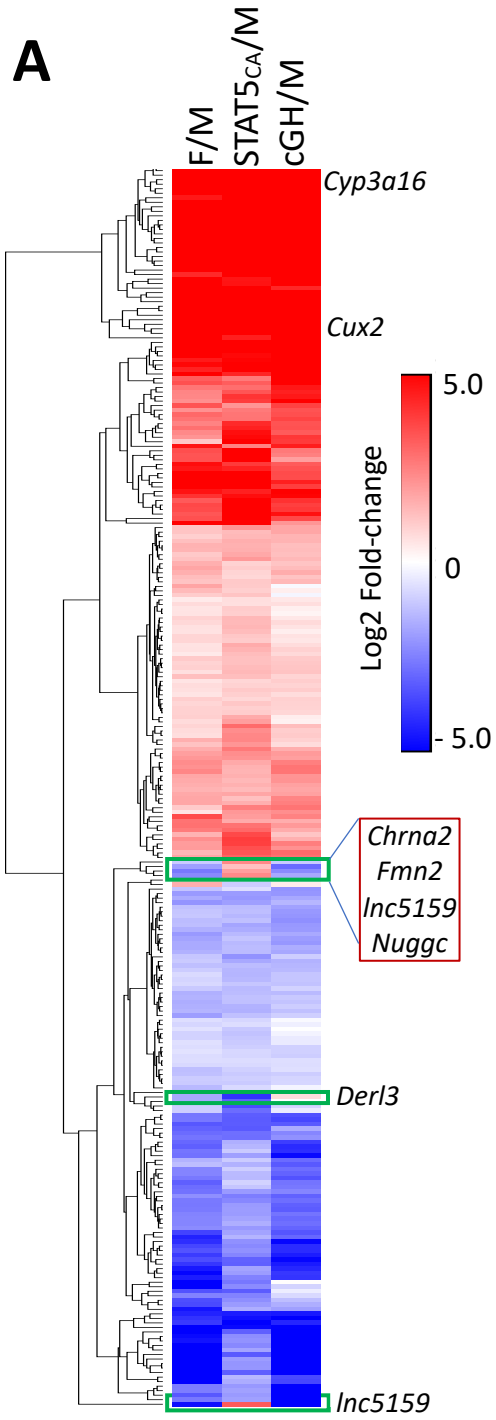
A
F/M
STAT5CA/M
cGH/M
Cyp3a16
Cux2
5.0
0
- 5.0
Log2 Fold-change
Chrna2
Fmn2
lnc5159
Nuggc
Derl3
lnc5159

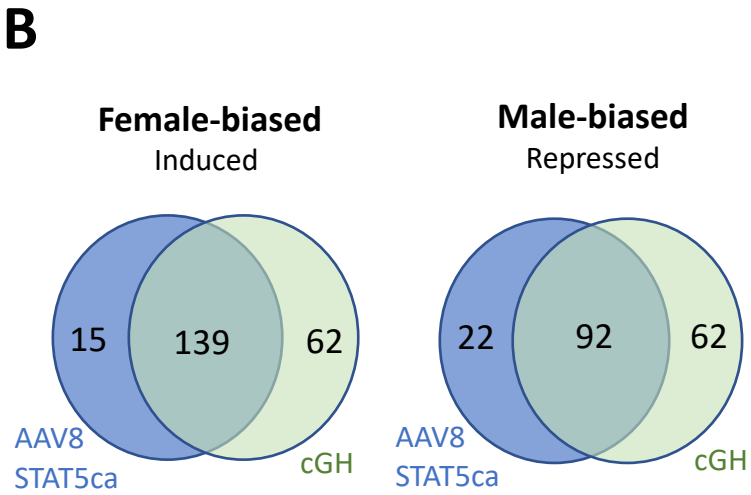
B
Female-biased
Induced
15
139
62
AAV8
STAT5ca
cGH
Male-biased
Repressed
22
92
62
AAV8
STAT5ca
cGH

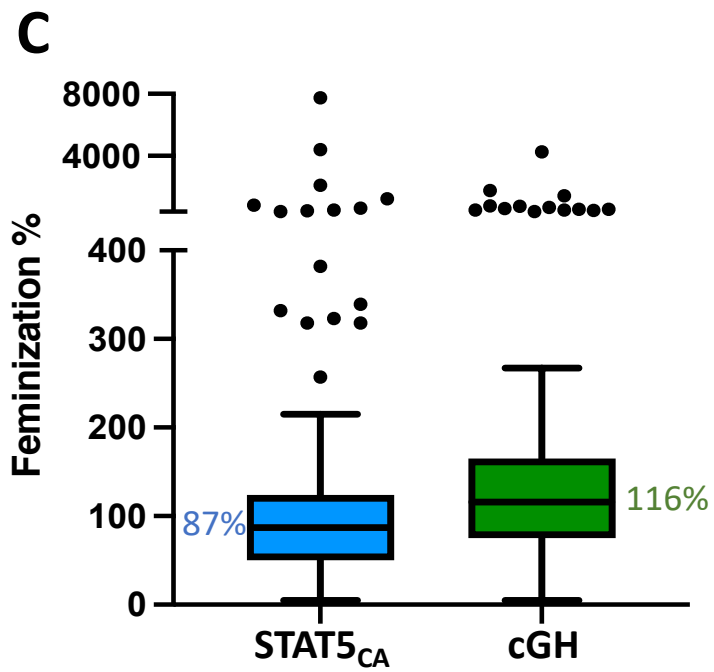
C
8000
4000
400
300
200
100
0
Feminization %
87%
116%
STAT5CA
cGH

Fig. 4

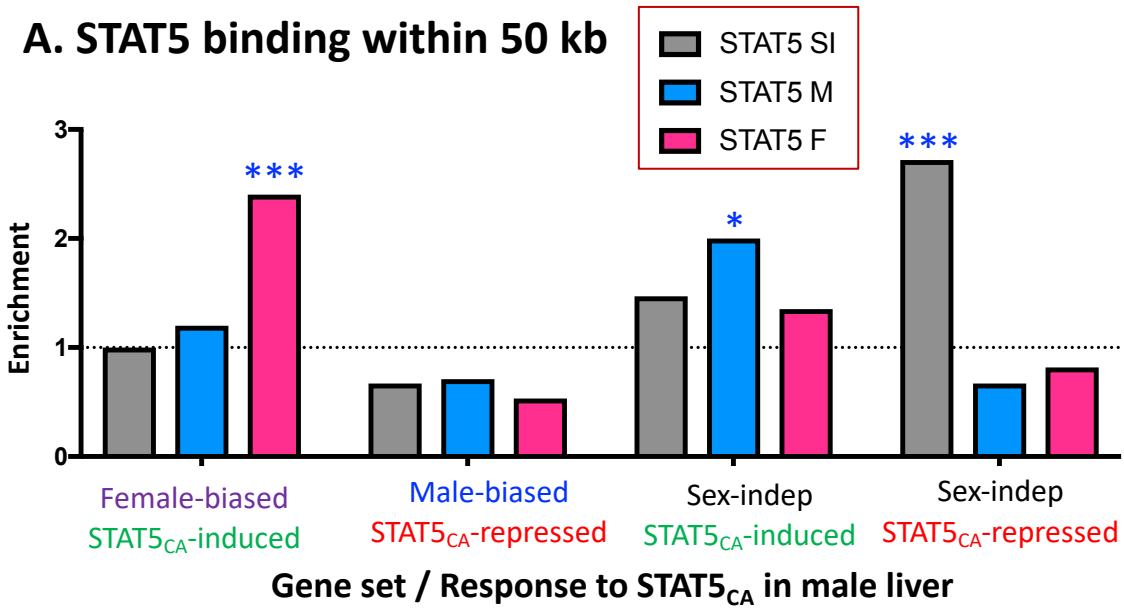
A. STAT5 binding within 50 kb
STAT5 SI
STAT5 M
STAT5 F
Enrichment
0
1
2
3
***
*
***
Female-biased
STAT5CA-induced
Male-biased
STAT5CA-repressed
Sex-indep
STAT5CA-induced
Sex-indep
STAT5CA-repressed
Gene set / Response to STAT5CA in male liver

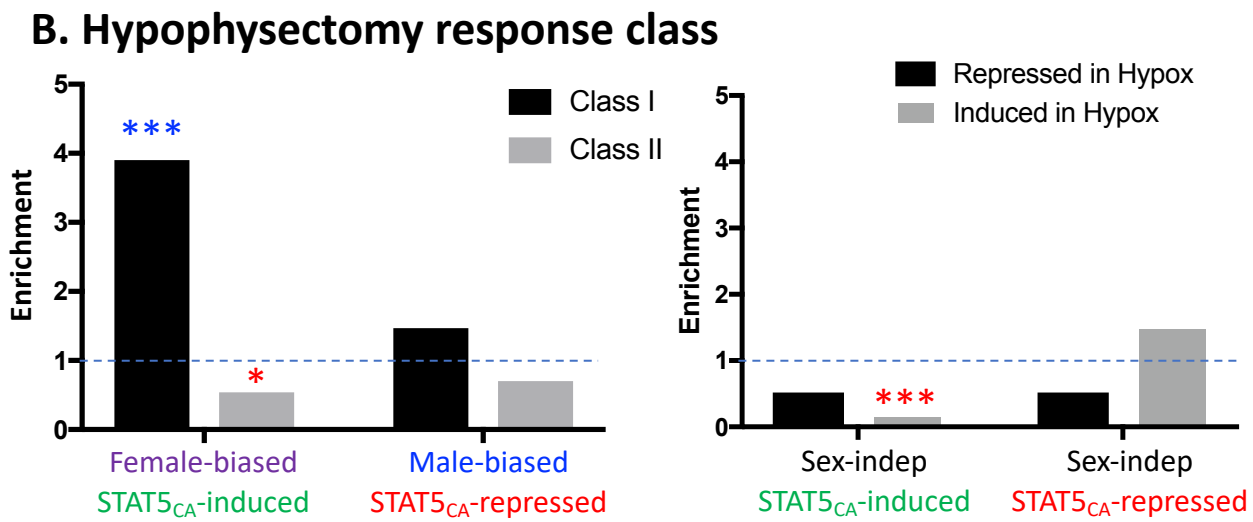
B. Hypophysectomy response class
Class I
Class II
Enrichment
0
1
2
3
4
5
***
*
Female-biased
STAT5CA-induced
Male-biased
STAT5CA-repressed
Repressed in Hypox
Induced in Hypox
***
Sex-indep
STAT5CA-induced
Sex-indep
STAT5CA-repressed

Fig. 5

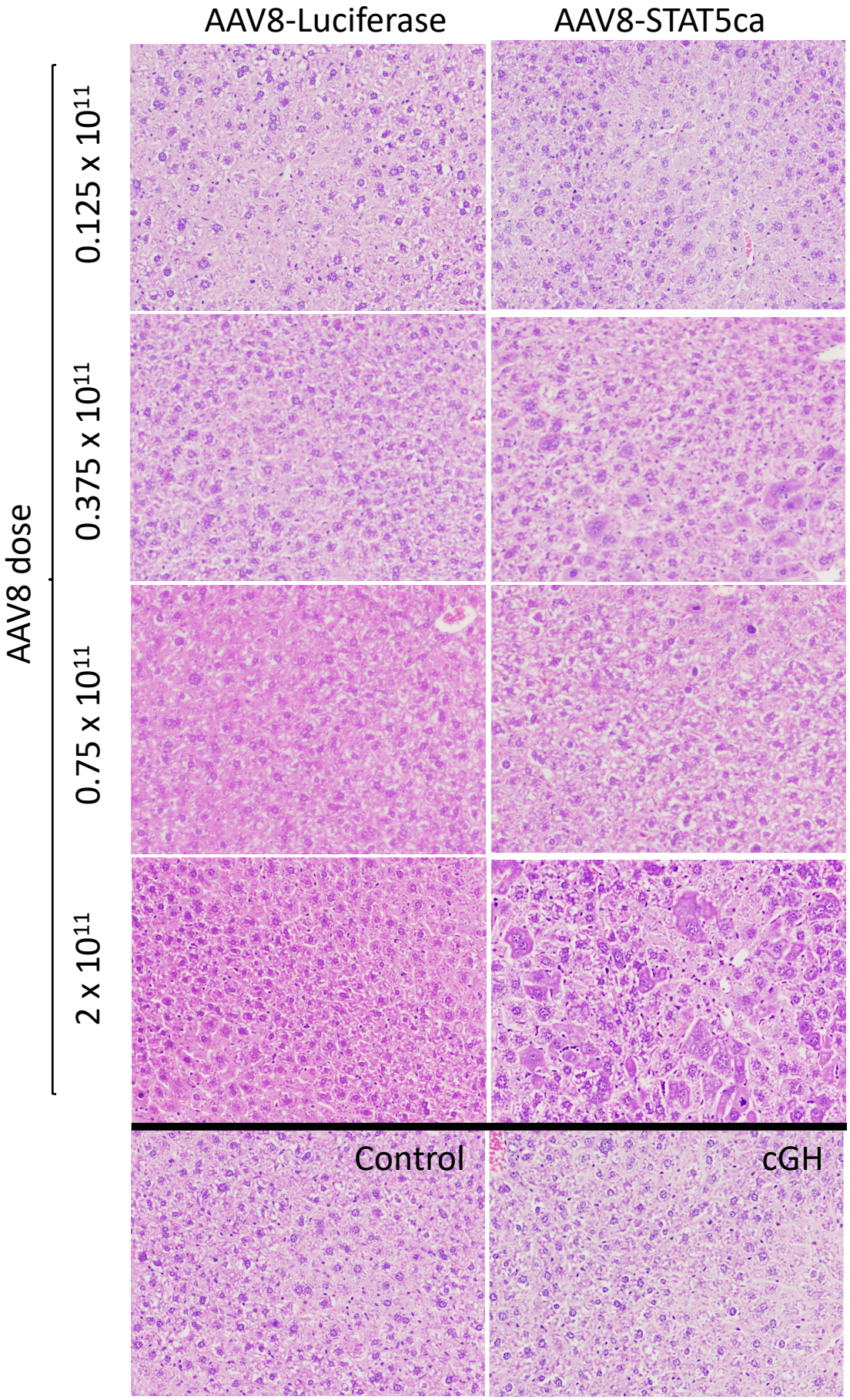
AAV8-Luciferase
AAV8-STAT5ca
AAV8 dose
0.125 x 10^11
0.375 x 10^11
0.75 x 10^11
2 x 10^11
Control
cGH

Fig. 6

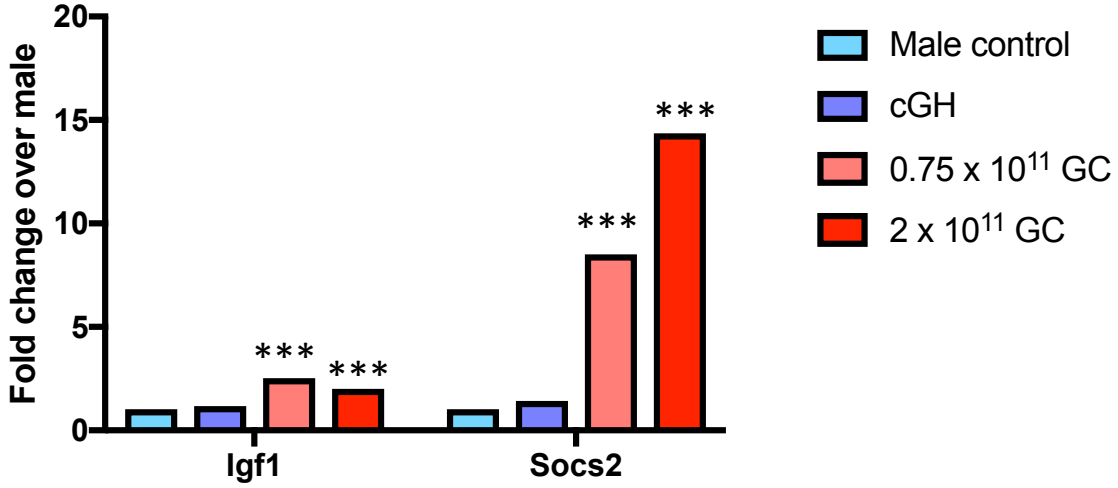
Fold change over male
20
15
10
5
0
***
***
***
***
Igf1
Socs2
Male control
cGH
0.75 x 10^11 GC
2 x 10^11 GC